JACS
JOURNAL OF THE AMERICAN CHEMICAL SOCIETY

Article

pubs.acs.org/JACS

Unveiling a New Aspect of Simple Arylboronic Esters: Long-Lived Room-Temperature Phosphorescence from Heavy-Atom-Free Molecules

Yoshiaki Shoji,[†,‡] Yasuhiro Ikabata,[‡,§] Qi Wang,[#,∥] Daisuke Nemoto,[†] Atsushi Sakamoto,[†] Naoki Tanaka,[†] Junji Seino,[#,∥] Hiromi Nakai,*[,§,#,∥,⊥] and Takanori Fukushima*[,†]

[†]Laboratory for Chemistry and Life Science, Institute of Innovative Research, Tokyo Institute of Technology, 4259 Nagatsuta, Midori-ku, Yokohama 226-8503, Japan

[§]Department of Chemistry and Biochemistry, School of Advanced Science and Engineering, and [#]Research Institute for Science and Engineering, Waseda University, Shinjuku, Tokyo 169-8555, Japan

[∥]CREST, Japan Science and Technology Agency, Kawaguchi, Saitama 332-0012, Japan

[⊥]Elements Strategy Initiative for Catalysts and Batteries (ESICB), Kyoto University, Saikyo-ku, Kyoto 615-8245, Japan

Supporting Information

ABSTRACT: Arylboronic esters can be used as versatile reagents in organic synthesis, as represented by Suzuki–Miyaura cross-coupling. Here we report a serendipitous finding that simple arylboronic esters are phosphorescent in the solid state at room temperature with a lifetime on the order of several seconds. The phosphorescence properties of arylboronic esters are remarkable in light of the general notion that phosphorescent organic molecules require heavy atoms and/or carbonyl groups for the efficient generation of a triplet excited state. Theoretical calculations on phenylboronic acid pinacol ester indicated that this molecule undergoes an out-of-plane distortion at the (pinacol)B–C_{ipso} moiety in the T_1 excited state, which is responsible for its phosphorescence. A compound survey with 19 arylboron compounds suggested that the phosphorescence properties might be determined by solid-state molecular packing rather than by the patterns and numbers of boron substituents on the aryl units. The present finding may update the general notion of phosphorescent organic molecules.

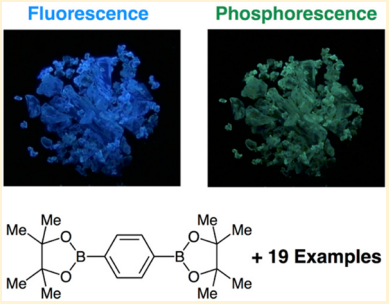

INTRODUCTION

Precious metal-free organic compounds that exhibit room-temperature phosphorescence have recently attracted considerable attention because of their high potential for the development of efficient and low-cost luminescent materials, which may lead to a variety of applications, including biological imaging as well as electroluminescent and sensing devices.[1] Phosphorescence occurs via spin-forbidden transitions;[2] a molecule in the excited singlet state (S_1) undergoes intersystem crossing to generate the lowest excited triplet state (T_1), and phosphorescence emission then takes place through a radiative transition from T_1 to the ground state (S_0). In general, unless molecules contain heavy atoms, these spin-forbidden transitions are very inefficient. In such a case, nonradiative decay due to molecular motion and intermolecular collisions becomes predominant. Hence, organic molecules that lack heavy atoms scarcely emit phosphorescence at room temperature. One approach to achieving room-temperature phosphorescence with heavy-atom-free molecules is to embed them in a solid matrix, so that the molecules can be isolated and structurally fixed to suppress nonradiative decay.[3] Meanwhile, several precious metal-free organic molecules have recently been reported to exhibit room-temperature phosphorescence in the solid state.[4] For example, Kim and co-workers showed that benzene derivatives with formyl and Br groups can emit phosphorescence at room temperature in the solid state with a lifetime on the order of a millisecond (τ = 5.4 ms).[4b] It has been considered that the attachment of carbonyl groups and heavy halogen atoms (Br and I) to the aromatic skeleton facilitates spin–orbit coupling, thus promoting both S_1-to-T_1 intersystem crossing and the subsequent radiative T_1-to-S_0 transition of phosphorescence.[4b]

During our synthetic study of π-conjugated molecules and polymers using Suzuki–Miyaura cross-coupling,[5] we noticed that 1,4-benzenediboronic acid bis(pinacol)ester **1** (Figure 1a), a common reagent in this cross-coupling protocol, displayed long-lived room-temperature phosphorescence in the solid state. Upon irradiation with UV light (λ = 254 nm) from a benchtop UV lamp, a crystalline sample of **1** exhibited blue-colored luminescence in air at 298 K (Figure 1b). Surprisingly, after the UV lamp was turned off, this sample showed a green-colored emission, which lasted for several seconds (Figure 1b).[6] This unexpected finding prompted us to further investigate the

Received: November 20, 2016
Published: January 30, 2017

DOI: 10.1021/jacs.6b11984
J. Am. Chem. Soc. 2017, 139, 2728–2733

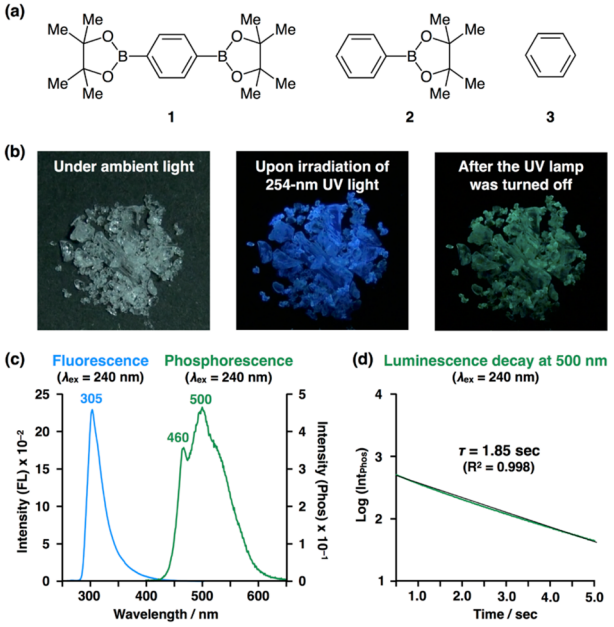

Figure 1. (a) Molecular structures of 1,4-benzenediboronic acid bis(pinacol)ester (**1**), phenylboronic acid pinacol ester (**2**), and benzene (**3**). (b) Photographs of a crystalline sample of **1** under ambient light (left), under irradiation with 254 nm UV light in the dark (middle), and after the UV light was turned off in the dark (right). (c) Fluorescence and phosphorescence spectra (λ_{ex} = 240 nm) and (d) phosphorescence decay profile at λ = 500 nm of a crystalline sample of **1** sandwiched between KBr plates in air at 298 K.

emission properties of **1** as well as those of structurally related simple arylboron compounds (18 examples). Herein, we report the results of the compound survey, along with theoretical calculations on the ground and excited states of phenylboronic acid pinacol ester **2** as a model (Figure 1a).

RESULTS AND DISCUSSION

Emission Properties of Arylboronic Esters. As shown in Figure 1c, a crystalline sample of **1** sandwiched between KBr plates at 298 K exhibited a delayed luminescence at a longer wavelength region (λ_{max} = 460 and 500 nm) with a lifetime (τ) of 1.85 s (quantum yield $\Phi \approx 2.0\%$),[7] along with fluorescence at λ_{max} = 305 nm (λ_{ex} = 240 nm) with a much shorter lifetime (τ = 7.8 ns). The lifetime of the delayed luminescence is exceptionally long for organic compounds (Figure 1d).[4] The delayed luminescence was not observed when a ground powder sample of **1** was measured in the presence of O_2, while the fluorescence from this sample remained intact. Thus, the long-lived luminescence of **1** is considered to be phosphorescence.[2] Under atmospheric conditions, the intensity of the phosphorescence from a crystalline sample of **1** decreased monotonically, while the spectral shape was maintained (Figure S5). Accordingly, the room-temperature phosphorescence of **1** occurs from a single radiative process. As expected, the crystalline sample of **1** at 77 K exhibited phosphorescence (λ_{max} = 464 and 495 nm, λ_{ex} = 255 nm, Figure S6) with an even longer lifetime (τ = 3.45 s, $\Phi_{Phos} \approx 13.1\%$).[7] While an ethanol solution of **1** (1.5×10^{-5} M) was not phosphorescent at 298 K under argon, its glass state at 77 K exhibited phosphorescence (λ_{max} = 375, 390, 400, 414, and 426 nm, λ_{ex} = 235 nm) with a significantly long lifetime (τ = 12.6 s, $\Phi_{Phos} \approx 50.1\%$)[7] (Figure S7). Considering the fact that nonsubstituted benzene (**3**) in a glass ethanol at 77 K shows a much shorter phosphorescence lifetime (τ = 7.7 s),[8] the boronic ester group of **1** likely plays a key role in suppressing the nonradiative transition from the T_1 state to the ground state (S_0).

We confirmed that the single-crystal X-ray structure of **1** is identical to that reported previously,[9] where two crystallographically independent molecules form a herringbone-type structure (Figure S1). Close intermolecular contact was not observed between the central phenylene ring of each molecule (e.g., the shortest intermolecular C_{Ar}–C_{Me} distance = 3.707 Å), possibly due to the steric bulk of the pinacol ester groups. According to the X-ray structure of **1**, there is no notable feature that could be expected to lead to room-temperature phosphorescence. Simply, molecular motion, which is related to the nonradiative decay of excited states, seems to be suppressed in the crystal.

Interestingly, a crystalline sample of monosubstituted phenylboronic acid pinacol ester **2** (Figure 1a) also exhibited

Table 1. $\pi \rightarrow \pi^*$ Excitation Properties of 2 and Benzene 3 Calculated at the TD-ωB97X-D/6-311G(d,p) Level[a]

2	ΔE (eV)	λ (nm)	f	Configuration (orbital symmetry)	Coefficient
$S_0(1^1A) \rightarrow S_1(1^1B)$	5.331	232.6	0.009	HOMO−1 (30a) → LUMO (26b)	0.576
				HOMO (25b) → LUMO+1 (31a)	0.403
$S_0(1^1A) \rightarrow S_2(2^1A)$	5.925	209.2	0.218	HOMO (25b) → LUMO (26b)	0.640
				HOMO−1 (30a) → LUMO+1 (31a)	−0.289
$S_0(1^1A) \rightarrow S_3(2^1B)$	6.948	178.5	0.112	HOMO−2 (29a) → LUMO (26b)	0.435
				HOMO (25b) → LUMO+1 (31a)	0.393
$S_0(1^1A) \rightarrow S_4(3^1A)$	6.991	177.3	0.866	HOMO−1 (30a) → LUMO+1 (31a)	0.633
				HOMO (25b) → LUMO (26b)	0.283
Benzene **3**	ΔE (eV)	λ (nm)	f	Configuration (orbital symmetry)	Coefficient
$S_0(1^1A_{1g}) \rightarrow S_1(1^1B_{2u})$	5.600	221.4	0.000	HOMO ($1e_{1g}$) → LUMO ($1e_{2u}$)	0.500
				HOMO−1 ($1e_{1g}$) → LUMO+1 ($1e_{2u}$)	0.500
$S_0(1^1A_{1g}) \rightarrow S_2(1^1A_{1u})$	6.349	195.3	0.000	HOMO−1 ($1e_{1g}$) → LUMO ($1e_{2u}$)	−0.497
				HOMO ($1e_{1g}$) → LUMO+1 ($1e_{2u}$)	0.498
$S_0(1^1A_{1g}) \rightarrow S_3(1^1E_{1u})$	7.362	168.4	0.605	HOMO−1 ($1e_{1g}$) → LUMO+1 ($1e_{2u}$)	0.498
				HOMO ($1e_{1g}$) → LUMO ($1e_{2u}$)	−0.498
$S_0(1^1A_{1g}) \rightarrow S_4(1^1E_{1u})$	7.362	168.4	0.605	HOMO−1 ($1e_{1g}$) → LUMO ($1e_{2u}$)	0.499
				HOMO (1e1g) → LUMO+1 ($1e_{2u}$)	0.497

[a] ΔE, λ, and f represent the singlet excitation energy, wavelength, and oscillation strength, respectively.

DOI: 10.1021/jacs.6b11984
J. Am. Chem. Soc. 2017, 139, 2728−2733

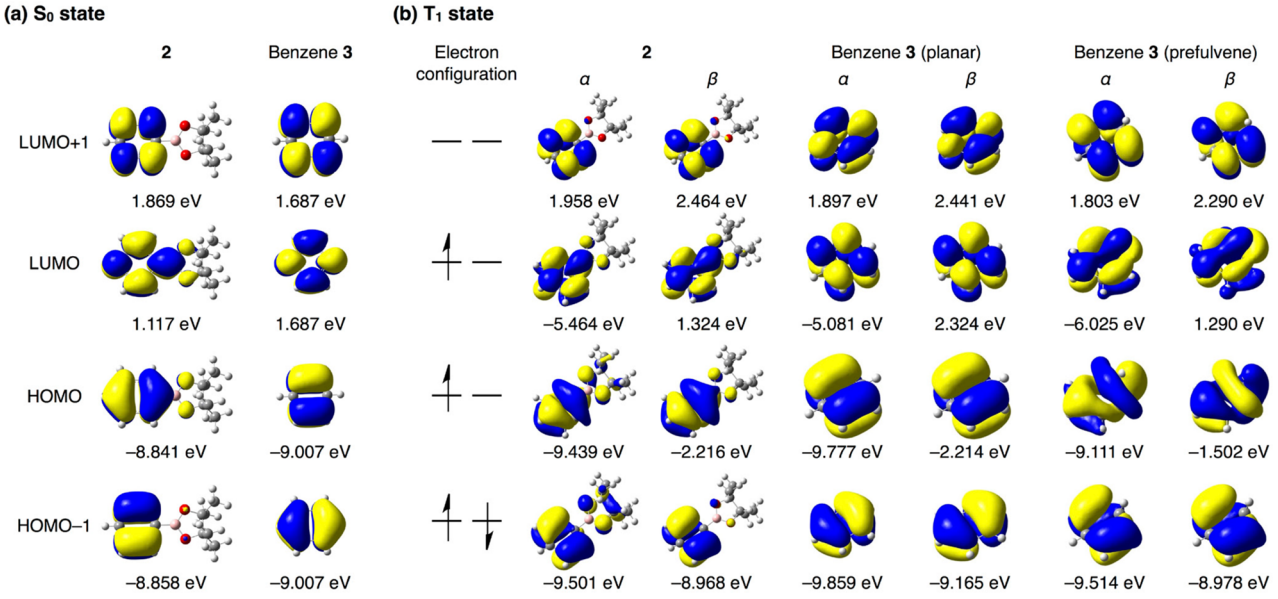

Figure 2. Frontier orbitals of (a) **2** and benzene **3** at the S_0 geometries, and of (b) **2** and benzene **3** (planar and prefulvene) at the T_1 geometries calculated at the (U)ωB97X-D/6-311G(d,p) level.

phosphorescence (λ_{max} = 465 nm, λ_{ex} = 245 nm) at 298 K, and the lifetime (τ = 1.79 s) was comparable to that for **1** (τ = 1.85 s) under identical measurement conditions (Figure S8). Previously, boronic ester-appended tellurophenes have been reported to show room-temperature phosphorescence upon aggregation.[10] The phosphorescence properties were accounted for in terms of the heavy atom effect of tellurium, whereas the effect of the boronic ester group on the phosphorescent properties has not been noted.[10]

Theoretical Calculations. To understand the unexpected phosphorescence properties of **1** and **2**, we investigated the substituent effect of the boronic ester on the absorption and emission properties of benzene using theoretical calculations. Table 1 and Figure 2 show the absorption energies and frontier orbitals of **2** and benzene **3**, respectively. The excitation properties were calculated using the S_0-optimized geometries of **2** and benzene **3**,[6] where the vertical excitation approach was used on the basis of the Franck−Condon principle. Similar $\pi \rightarrow \pi^*$ excitation nature was observed in all of the selected excitations. The calculated $S_0 \rightarrow S_1$ and $S_0 \rightarrow S_2$ excitation energies (ΔE, Table 1) are in good agreement with the previously reported experimental values.[11] The calculated oscillator strength (f) shows that the $S_0 \rightarrow S_1$ and $S_0 \rightarrow S_2$ excitations of **2** are allowed, while those of **3** are forbidden, which is consistent with the symmetries of the electronic states. The vibronic effect[12] seems to be important for reproducing the low-lying excitation peaks of benzene. As shown in Figure 2, degenerate LUMO and LUMO+1 orbitals were observed for benzene **3** at 1.687 eV. On the other hand, the LUMO level of **2** (1.117 eV) was approximately 0.5 eV lower than that of **3**, as a result of the interaction between π^*(phenyl) and vacant 2p(boron) orbitals, where the boron serves as a π-acceptor. The LUMO+1 level of **2** (1.869 eV) was approximately 0.2 eV higher than that of benzene **3** (1.687 eV). The energy levels of the nearly degenerate HOMO and HOMO−1 of **2** (−8.841 and −8.858 eV) were close to those of **3** (−9.007 eV). Consequently, the HOMO−LUMO gap and the excitation energies of **2** became lower than those of **3** (Table 1 and Figure 2).

The calculated singlet−triplet energy difference [$\Delta E(T_1-S_0)$] in Table 2 was obtained at the T_1-optimized geometries

Table 2. Calculated Phosphorescent Properties of 2 and Benzene 3 at the (U)ωB97X-D/6-311G(d,p) Level

	ΔE (T_1-S_0) (eV)	λ_{calcd} (nm)	λ_{exp} (nm)
2	2.607	475.6	465[a]
3 (Planar)	3.306	375.0	337[b]
3 (Prefulvene)	1.585	782.1	−−

[a]Value obtained for a crystalline sample sandwiched between KBr plates at 298 K (Figure S8). [b]Value previously reported for benzene in a C_6D_6 host crystal at 4.2 K (ref 13).

(Tables S4, S5, and S8) on the basis of the Franck−Condon principle. The results were consistent with the previously reported experimental values.[13] Notably, the geometry of the T_1 state of **2** was much different from that of the S_0 state, where a significant out-of-plane distortion of the (pinacol)B−C_{ipso} moiety occurs with respect to the mean plane of the other carbon atoms in the equilibrium T_1 structure (Figures 2 and 3). This is in contrast to the case of benzene **3**, where two minima exist in the T_1 state; one is nonplanar (prefulvene), and the other is planar (Figures 2 and 3). Frontier orbitals for the T_1 geometries of **2**, **3** (planar), and prefulvene are summarized in Figure 2b. While **3** (planar) shows only π and π^* frontier orbitals, **2** and **3** (prefulvene) feature mixed-type orbitals in the T_1 states. As shown in Table 2, the phosphorescence properties of benzene **3** were derived from the planar T_1 geometry. Figure 3a schematically illustrates the transition from the T_1 state to the S_0 state of **2**. The $T_1 \rightarrow S_0$ transition can approximately be interpreted as an electronic transition (spin-flip transition) from the highest occupied α orbital to the lowest unoccupied β orbital of **2**. This transition process also involves a significant change in the molecular orbitals, particularly regarding whether or not an orbital interaction between the B and C_{ipso} atoms exists (Figure 3a).

From the perspective of energetics, the planar T_1 state of benzene **3** is stable only at low temperature. When environ-

DOI: 10.1021/jacs.6b11984
J. Am. Chem. Soc. 2017, 139, 2728−2733

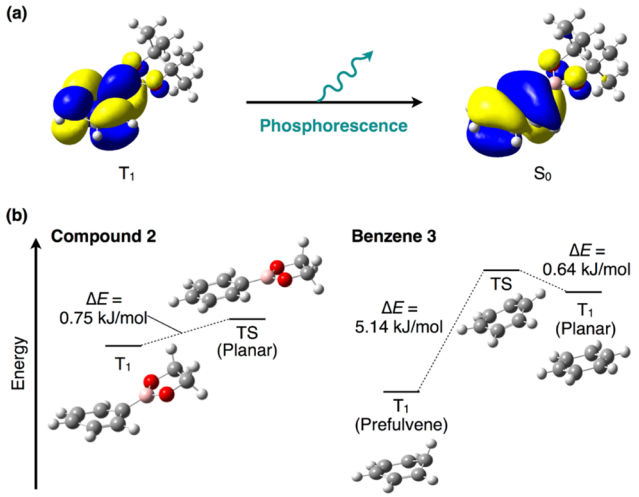

Figure 3. (a) Schematic illustration of the phosphorescence emission process and the Kohn–Sham orbitals of **2** in the T_1 (−5.464 eV, Figure 2b) and S_0 states. The orbital of the S_0 state was obtained using the T_1-optimized geometry on the basis of the Franck–Condon principle. (b) Energy diagrams of **2** and benzene **3** in the T_1 states obtained by TD-DFT calculations at the UωB97X-D/6-311G(d,p) level.

mental (thermal) fluctuation increases, the planar T_1 state of benzene is expected to easily surpass the energy barrier, and consequently, the nonplanar prefulvene should become dominant (Figure 3b). On the other hand, the planar T_1 structure of **2** is a transition state structure, which could easily lead to the nonplanar equilibrium point (Figure 3b). Therefore, a sustained molecular out-of-plane distortion could be expected for **2** even at room temperature. This out-of-plane distortion may facilitate the mixing of π and σ orbitals,[14] which likely contributes to the spin–orbit coupling for intersystem crossing between the singlet and triplet states.[15]

To investigate how the molecular distortion affects the phosphorescence emission ability of **2** and **3**, we calculated the spin–orbit coupling constant (SOC) using a multireference perturbation method.[6] Table 3 shows the S_0–T_1 energy gaps,

Table 3. Results of Multireference Perturbation Calculations of Phosphorescence Properties of 2 and 3 Using CASSCF(6,6) Wavefunction and 6-311G(d,p) Basis Set

	ΔE (T_1–S_0) (eV)	λ_{calcd} (nm)	S_0/T_1 SOC (cm^{-1})
2	2.837	437.1	2.13
3 (Planar)	3.268	379.5	0.00
3 (Prefulvene)	1.553	798.5	0.18

corresponding wavelengths, and S_0/T_1 SOCs at the T_1 equilibrium geometries of **2** and **3**. The energy gaps and phosphorescence wavelengths are similar to the values listed in Table 2. The SOC value of planar **3** was zero, while those of nonplanar **2** and prefulvene **3** were nonzero. Notably, the absolute SOC value of nonplanar **2** (2.13 cm^{-1}) is significantly larger than that of prefulvene **3** (0.18 cm^{-1}). From these results, we conclude that the structural deformation at the T_1 state is responsible for nonzero SOC, and the boron functionality is able to not only stabilize the distorted structure of benzene chromophore (Figure 3) but also increase S_0/T_1 SOC, resulting in facilitating the phosphorescent process.

Compound Survey. A compound survey using arylboronic esters (**4**–**18**) as well as related boron compounds (**19** and **20**) revealed that the long-lived phosphorescence from boron species is not a special phenomenon. Indeed, 14 of the total 19 arylboron compounds emitted long-lived phosphorescence at room temperature in the solid state. Figure 4 and Table 4 show

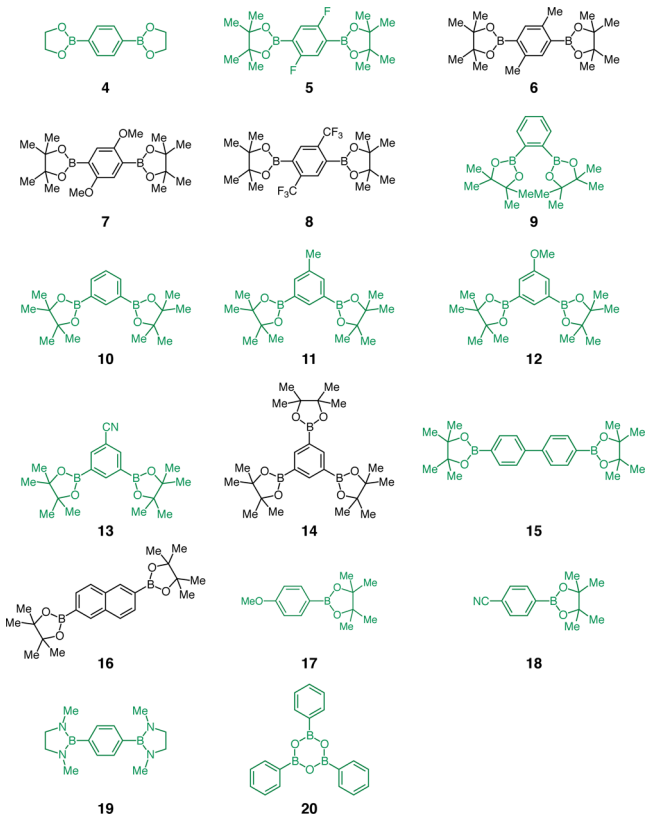

Figure 4. Molecular structures of boron compounds used for the compound survey. Green-colored compounds emit clear phosphorescence, and black-colored compounds are scarcely phosphorescent at room temperature in the solid state.

the molecular structures of the boron compounds examined and the luminescence data of their crystalline samples at 298 K, respectively.[6] A simple 1,4-disubstituted benzene with 1,3-dioxaboron-2-yl (**4**) groups showed phosphorescence with τ = 1.65 s (Figure S9). A 1,4-benzenediboronic acid bis(pinacol)-ester with fluoro groups (**5**) was also phosphorescent (Figure S10). In sharp contrast, its analogues **6**, **7**, and **8**, which carry methyl, methoxy, and trifluoromethyl groups, respectively, were scarcely phosphorescent under the measurement conditions at room temperature (Figures S11–S13). Presumably, the attachment of the relatively bulky groups to the central benzene ring might increase the free volume around the boron functionality in the crystal, which could allow a molecular motion that leads to thermal deactivation of the excited state. Bis(pinacol)esters of 1,2- and 1,3-benzenediboronic acids (**9** and **10**) serve as a room-temperature phosphor (Figures S14 and S15). Interestingly, unlike the 1,4-diborylated versions, the attachment of methyl (**11**), methoxy (**12**), and cyano (**13**) groups to 1,3-diborylated benzenes did not impair the room-temperature phosphorescence properties, regardless of the electron-donating or -accepting nature of the substituent (Figures S16–S18). However, no phosphorescence from a 1,3,5-triborylated version (**14**) was observed (Figure S19). A

DOI: 10.1021/jacs.6b11984
J. Am. Chem. Soc. 2017, 139, 2728–2733

Table 4. Emission Properties of Boron Compounds in the Solid State at 298 K (KBr)[a]

	λ_{FL} (nm)	λ_{Phos} (nm)	τ_{Phos} (s)
4	316	471, 506	1.65
5	351	507	0.56
6	328	528 (very weak)	n.d.[c]
7	385	514 (very weak)	n.d.[c]
8	301	456 (very weak)	n.d.[c]
9	302	500	1.73
10	297	469, 500	1.57
11	305	452,478	0.49
12	329	480	0.69
13	306	449, 473	0.42
14	306	n.d.[b]	n.d.[c]
15	343	536	0.20
16	360, 378	n.d.[b]	n.d.[c]
17	298	502	1.39
18	306	519	0.44
19	400	457	0.79
20	302	461, 495	0.46

[a]The spectral data are shown in Figures S8–S25. [b]Not detected. [c]Not determined.

bis(pinacol)ester of 4,4′-biphenyldiboronic acid (**15**) was phosphorescent at room temperature (Figure S20), while the lifetime was shorter than that of **1**. In contrast, 2,6-naphthalenediboronic acid bis(pinacol)ester (**16**) was scarcely phosphorescent (Figure S21), implying that even with boronic ester groups, highly fluorescent aromatic compounds might not be able to emit phosphorescence efficiently. Monoborylated compounds **17** and **18** with electron-donating and -accepting substituents, respectively, likewise exhibited room-temperature phosphorescence (Figures S22 and S23). Since 1,4-disubstituted benzene with 1,3-dimethyl-1,3-diazaborolidin-2-yl groups (**19**) can emit phosphorescence at room temperature, the oxygen atoms attached to boron do not seem to be essential for the room-temperature phosphorescence properties (Figure S24). Notably, a simple boroxine (**20**) also displayed phosphorescence at room temperature (Figure S25). Considering that boroxine derivatives have been used as a scaffold for various supramolecular architectures,[16] this observation may stimulate the exploration of new photophysical functions of boroxine-containing supramolecular materials. Also notably, a powder sample of hexagonal boron nitride,[17] which is referred to as an inorganic graphite, was found to emit a long-lived (τ = 1.58 s) room-temperature luminescence at λ = 441 nm (Figure S26).

X-ray Diffraction Analysis. In our compound survey, there was no particular tendency regarding the substitution patterns or numbers of boron functionalities on aryl units. Therefore, we closely compared the crystal structures of phosphorescent molecules (**1**,[9] **4**, and **5**) and scarcely phosphorescent **6** (Figures S1–S4).[6] However, the common structural features in the phosphorescent molecules as well as the difference between the phosphorescent molecules and scarcely phosphorescent **6** remain elusive. For instance, **6** forms a herringbone-type structure similar to **1** and **5**, where the aromatic ring of each compound is almost coplanar with the trigonal planes of the boron functionality. Intermolecular van der Waals contacts involving the central aryl units are present for **5** and **6**, but absent for **1**. Although **4** does not adopt a herringbone-type structure, it can emit phosphorescence efficiently.

CONCLUSIONS

In summary, we have demonstrated that simple arylboron compounds exhibit room-temperature phosphorescence in the solid state. The phosphorescence lifetimes are on the order of several seconds, which is exceptionally long for organic compounds. Detailed theoretical calculations on phenylboronic acid pinacol ester (**2**) indicated that the molecule undergoes an out-of-plane distortion at the (pinacol)B–C_{ipso} moiety in the excited T_1 state. This deformation may facilitate the mixing of π and σ orbitals that promotes spin–orbit coupling, which in turn likely contributes to the phosphorescent properties even at room temperature. We do not currently know the structural features of boron compounds capable of emitting room-temperature phosphorescence in the solid state. Nevertheless, we believe that the new aspect of simple boron compounds unveiled in this study may not only stimulate fundamental science on the photophysical properties of organic molecules, but could also inspire the design of heavy-atom-free phosphorescent materials.

ASSOCIATED CONTENT

Supporting Information

The Supporting Information is available free of charge on the ACS Publications website at DOI: 10.1021/jacs.6b11984.

Experimental and computational details and data (PDF)
Crystallographic data for **4**-**6** (CIF)

AUTHOR INFORMATION

Corresponding Authors

*nakai@waseda.jp (H.N.)
*fukushima@res.titech.ac.jp (T.F.)

ORCID

Hiromi Nakai: 0000-0001-5646-2931
Takanori Fukushima: 0000-0001-5586-9238

Author Contributions

‡Y.S. and Y.I. contributed equally.

Notes

The authors declare no competing financial interest.

ACKNOWLEDGMENTS

This work was supported by KAKENHI (Nos. 26102008 and 26708004) and "Dynamic Alliance for Open Innovation Bridging Human, Environment and Materials" from the Ministry of Education, Culture, Sports, Science and Technology of Japan (MEXT). The authors would like to thank Suzukakedai Materials Analysis Division, Technical Department, Tokyo Institute of Technology, for their support with the elemental analysis and ICP-AES analysis. The authors would also like to acknowledge JASCO Corporation for determining the phosphorescence quantum yields of **1**, A. Saeki (Osaka University) for measuring the time-dependent emission profile of **1**, and K. Yamamoto and K. Albrecht (Tokyo Institute of Technology) for their support with measuring the fluorescence lifetimes of boron compounds. Some of the present calculations were performed at the Research Center for Computational Science (RCCS), Okazaki Research Facilities, and National Institutes of Natural Sciences (NINS).

REFERENCES

(1) (a) Chaudhuri, D.; Sigmund, E.; Meyer, A.; Röck, L.; Klemm, P.; Lautenschlager, S.; Schmid, A.; Yost, S. R.; Van Voorhis, T.; Bange, S.;

DOI: 10.1021/jacs.6b11984
J. Am. Chem. Soc. 2017, 139, 2728–2733

Höger, S.; Lupton, J. M. *Angew. Chem., Int. Ed.* **2013**, *52*, 13449. (b) Thomas, S. W., III; Yagi, S.; Swager, T. M. *J. Mater. Chem.* **2005**, *15*, 2829. (c) Zhang, G.; Palmer, G. M.; Dewhirst, M. W.; Fraser, C. L. *Nat. Mater.* **2009**, *8*, 747. (d) Bergamini, G.; Fermi, A.; Botta, C.; Giovanella, U.; Di Motta, S.; Negri, F.; Peresutti, R.; Gingras, M.; Ceroni, P. *J. Mater. Chem. C* **2013**, *1*, 2717. (e) Yoshii, R.; Hirose, A.; Tanaka, K.; Chujo, Y. *J. Am. Chem. Soc.* **2014**, *136*, 18131. (f) Zheng, S.; Wang, X.; Mao, H.; Wu, W.; Liu, B.; Jiang, X. *Nat. Commun.* **2015**, *6*, 5834. (g) Sasabe, H.; Kido, J. *Eur. J. Org. Chem.* **2013**, *2013*, 7653.

(2) Turro, N. J.; Ramamurthy, V.; Scaianon, J. C. *Modern Molecular Photochemistry of Organic Molecules*; University Science Books: Sausalito, 2010.

(3) (a) Zhang, G.; Chen, J.; Payne, S. J.; Kooi, S. E.; Demas, J. N.; Fraser, C. L. *J. Am. Chem. Soc.* **2007**, *129*, 8942. (b) Al-Attar, H. A.; Monkman, A. P. *Adv. Funct. Mater.* **2012**, *22*, 3824. (c) Yong, G.; Zhang, X.; She, W. *Dyes Pigm.* **2013**, *97*, 65. (d) Lee, D.; Bolton, O.; Kim, B. C.; Youk, J. H.; Takayama, S.; Kim, J. *J. Am. Chem. Soc.* **2013**, *135*, 6325. (e) Kwon, M. S.; Yu, Y.; Coburn, C.; Phillips, A. W.; Chung, K.; Shanker, A.; Jung, J.; Kim, F.; Pipe, K.; Forrest, S. R.; Youk, J. H.; Gierschner, J.; Kim, J. *Nat. Commun.* **2015**, *6*, 8947. (f) Pang, X.; Wang, H.; Ran Zhao, X.; Jun Jin, W. *CrystEngComm* **2013**, *15*, 2722. (g) Kwon, M. S.; Lee, D.; Seo, S.; Jung, J.; Kim, J. *Angew. Chem., Int. Ed.* **2014**, *53*, 11177. (h) Bolton, O.; Lee, D.; Jung, J.; Kim, J. *Chem. Mater.* **2014**, *26*, 6644.

(4) (a) Mukherjee, S.; Thilagar, P. *Chem. Commun.* **2015**, *51*, 10988. (b) Bolton, O.; Lee, K.; Kim, H.-J.; Lin, K. Y.; Kim, J. *Nat. Chem.* **2011**, *3*, 205. (c) Xu, J.; Takai, A.; Kobayashi, Y.; Takeuchi, M. *Chem. Commun.* **2013**, *49*, 8447. (d) Koch, M.; Perumal, K.; Blacque, O.; Garg, J. A.; Saiganesh, R.; Kabilan, S.; Balasubramanian, K. K.; Venkatesan, K. *Angew. Chem., Int. Ed.* **2014**, *53*, 6378. (e) Kuno, S.; Akeno, H.; Ohtani, H.; Yuasa, H. *Phys. Chem. Chem. Phys.* **2015**, *17*, 15989. (f) Gong, Y.; Zhao, L.; Peng, Q.; Fan, D.; Yuan, W. Z.; Zhang, Y.; Tang, B. Z. *Chem. Sci.* **2015**, *6*, 4438. (g) Gong, Y.; Chen, G.; Peng, Q.; Yuan, W. Z.; Xie, Y.; Li, S.; Zhang, Y.; Tang, B. Z. *Adv. Mater.* **2015**, *27*, 6195. (h) Shimizu, M.; Shigitani, R.; Nakatani, M.; Kuwabara, K.; Miyake, Y.; Tajima, K.; Sakai, H.; Hasobe, T. *J. Phys. Chem. C* **2016**, *120*, 11631. (i) Shimizu, M.; Kimura, A.; Sakaguchi, H. *Eur. J. Org. Chem.* **2016**, *2016*, 467. (j) Zhao, W.; He, Z.; Lam, J. W. Y.; Peng, Q.; Ma, H.; Shuai, Z.; Bai, G.; Hao, J.; Tang, B. Z. *Chem.* **2016**, *1*, 592. (k) Fermi, A.; Bergamini, G.; Peresutti, R.; Marchi, E.; Roy, M.; Ceroni, P.; Gingras, M. *Dyes Pigm.* **2014**, *110*, 113. (l) Fermi, A.; Bergamini, G.; Roy, M.; Gingras, M.; Ceroni, P. *J. Am. Chem. Soc.* **2014**, *136*, 6395. (m) Yuan, W. Z.; Shen, X. Y.; Zhao, H.; Lam, J. W. Y.; Tang; Lu, P.; Wang, C.; Liu, Y.; Wang, Z.; Zheng, Q.; Sun, J. Z.; Ma, Y.; Tang, B. Z. *J. Phys. Chem. C* **2010**, *114*, 6090. (n) Wang, H.; Wang, H.; Yang, X.; Wang, Q.; Yang, Y. *Langmuir* **2015**, *31*, 486. (o) Li, D.; Tang, X.; Zhang, L.; Li, C.; Liu, Z.; Bo, Z.; Dong, Y. Q.; Tian, Y.-H.; Dong, Y.; Tang, B. Z. *Adv. Opt. Mater.* **2015**, *3*, 1184. (p) An, Z.; Zheng, X.; Tao, Y.; Chen, R.; Shi, H.; Chen, T.; Wang, Z.; Li, H.; Deng, R.; Liu, X.; Huang, W. *Nat. Mater.* **2015**, *14*, 685.

(5) Suzuki, A. *Angew. Chem., Int. Ed.* **2011**, *50*, 6723.

(6) See Supporting Information.

(7) The phosphorescence quantum yields of **1** were obtained on the basis of the area ratio of the emission spectrum in the photostationary state.

(8) (a) Leubner, I. H.; Hodgkins, J. E. *J. Phys. Chem.* **1969**, *73*, 2545. (b) Lumb, M. D.; Lloyd Braga, C.; Pereira, L. C. *Trans. Faraday Soc.* **1969**, *65*, 1992.

(9) Franz, D.; Bolte, M.; Lerner, H.-W.; Wagner, M. *Dalton Trans.* **2011**, *40*, 2433.

(10) He, G.; Delgado, W. T.; Schatz, D. J.; Merten, C.; Mohammadpour, A.; Mayr, L.; Ferguson, M. J.; McDonald, R.; Brown, A.; Shankar, K.; Rivard, E. *Angew. Chem., Int. Ed.* **2014**, *53*, 4587.

(11) Nakashima, N.; Inoue, H.; Sumitani, M.; Yoshihara, K. *J. Chem. Phys.* **1980**, *73*, 5976.

(12) Minaev, B. F.; Knuts, S.; Ågren, H.; Vahtras, O. *Chem. Phys.* **1993**, *175*, 245.

(13) Nieman, G. C.; Tinti, D. S. *J. Chem. Phys.* **1967**, *46*, 1432.

(14) (a) Penfold, T. J.; Worth, G. A. *Chem. Phys.* **2010**, *375*, 58. (b) Perun, S.; Tatchen, J.; Marian, C. M. *ChemPhysChem* **2008**, *9*, 282. (c) Marian, C. M.; Kleinschmidt, M.; Tatchen, J. *Chem. Phys.* **2008**, *347*, 346. (d) Kleinschmidt, M.; Marian, C. M. *Chem. Phys. Lett.* **2008**, *458*, 190. (e) Shchupak, E. E.; Ivashin, N. V.; Sagun, E. I. *Opt. Spectrosc.* **2013**, *115*, 37. (f) Rodriguez-Serrano, A.; Rai-Constapel, V.; Daza, M. C.; Doerra, M.; Marian, C. M. *Photochem. Photobiol. Sci.* **2012**, *11*, 1860.

(15) (a) Hirata, S.; Totani, K.; Zhang, J.; Yamashita, T.; Kaji, H.; Marder, S. R.; Watanabe, T.; Adachi, C. *Adv. Funct. Mater.* **2013**, *23*, 3386. (b) Reineke, S.; Baldo, M. A. *Sci. Rep.* **2014**, *4*, 3797. (c) Minaev, B.; Baryshnikov, G.; Agrena, H. *Phys. Chem. Chem. Phys.* **2014**, *16*, 1719.

(16) (a) Yang, H.; Du, Y.; Wan, S.; Trahan, G. D.; Jina, Y. *Chem. Sci.* **2015**, *6*, 4049. (b) Ding, S.-Y.; Wang, W.; Zhang, W. *Chem. Soc. Rev.* **2013**, *42*, 548. (c) Côté, A. P.; Benin, A. I.; Ockwig, N. W.; O'Keeffe, M.; Matzger, A. J.; Yaghi, O. M. *Science* **2005**, *310*, 1166. (d) El-Kaderi, H. M.; Hunt, J. R.; Mendoza-Cortés, J. L.; Côté, A. P.; Taylor, R. E.; O'Keeffe, M.; Yaghi, O. M. *Science* **2007**, *316*, 268. (e) Tokunaga, Y.; Ito, T.; Sugawara, H.; Nakata, R. *Tetrahedron Lett.* **2008**, *49*, 3449. (f) Chen, T.-H.; Kaveevivitchai, W.; Bui, N.; Miljanić, O. Š. *Chem. Commun.* **2012**, *48*, 2855. (g) Ono, K.; Johmoto, K.; Yasuda, N.; Uekusa, H.; Fujii, S.; Kiguchi, M.; Iwasawa, N. *J. Am. Chem. Soc.* **2015**, *137*, 7015.

(17) Hexagonal boron nitride was purchased from Wako Pure Chemical Industries (code: 028-02281, Lot No. LAQ5877) and used as received.

DOI: 10.1021/jacs.6b11984
J. Am. Chem. Soc. 2017, 139, 2728−2733